Density Functional Theory Analysis of the Reaction Pathway for Methane Oxidation to Acetic Acid Catalyzed by Pd^{2+} in Sulfuric Acid

Shaji Chempath and Alexis T. Bell*

Contribution from the Department of Chemical Engineering, University of California, Berkeley, California 94720-1462

Received August 22, 2005; E-mail: bell@cchem.berkeley.edu

Abstract: Density functional theory has been used to investigate the thermodynamics and activation barriers associated with the direct oxidation of methane to acetic acid catalyzed by Pd^{2+} cation in concentrated sulfuric acid. Pd^{2+} cations in such solutions are ligated by two bisulfate anions and by one or two molecules of sulfuric acid. Methane oxidation is initiated by the addition of CH$_4$ across one of the Pd$-$O bonds of a bisulfate ligand to form Pd(HSO$_4$)(CH$_3$)(H$_2$SO$_4$)$_2$. The latter species will react with CO to produce Pd-(HSO$_4$)(CH$_3$CO)(H$_2$SO$_4$)$_2$. The most likely path to the final products is found to be via oxidation of Pd-(HSO$_4$)(CH$_3$)(H$_2$SO$_4$)$_2$ and Pd(HSO$_4$)(CH$_3$CO)(H$_2$SO$_4$)$_2$ to form Pd(η^2-HSO$_4$)(HSO$_4$)$_2$(CH$_3$)(H$_2$SO$_4$) and Pd(η^2-HSO$_4$)(HSO$_4$)$_2$(CH$_3$CO)(H$_2$SO$_4$), respectively. CH$_3$HSO$_4$ or CH$_3$COHSO$_4$ is then produced by reductive elimination from the latter two species, and CH$_3$COOH is then formed by hydrolysis of CH$_3$COHSO$_4$. The loss of Pd^{2+} from solution to form Pd(0) or Pd-black is predicted to occur via reduction with CO. This process is offset, though, by reoxidation of palladium by either H$_2$SO$_4$ or O$_2$.

Introduction

The direct conversion of methane to other chemicals is a subject of continuing interest. One of the products that can be made by this means is acetic acid, a commodity chemical widely used in the chemical industry. Periana et al.[1] have reported that Pd^{2+} cations in 96% sulfuric acid will catalyze the direct oxidation of methane at 453 K to acetic acid, with methyl bisulfate (a precursor to methanol) and carbon dioxide as the only byproducts. It was observed, though, that during the course of the reaction Pd^{2+} is reduced and precipitates from solution as Pd-black, resulting in the loss of the active catalyst. The authors noted that while H$_2$SO$_4$ can oxidize metallic Pd back to Pd^{2+}, the rate at which the reaction proceeds is insufficient to maintain Pd in solution. Zerella and Bell[2] have confirmed these results and have shown that the retention of Pd^{2+} in solution is controlled by the balance between the oxidizing and reducing potentials of the reaction system. These investigators reported that, by adding oxygen to the methane feed and controlling the total reactant pressure, virtually all of the Pd^{2+} can be retained in solution. These conditions also lead to an enhancement in the yield of acetic acid relative to what is observed in the absence of oxygen.

Insights into the elementary processes involved in the activation and oxidation of methane catalyzed by Pt and Au cations in sulfuric acid have been gained from quantum chemical studies. Ziegler and co-workers[3,4] have studied the mechanism of methane activation and functionalization by Pt^{2+} in sulfuric acid and have concluded that methane activation occurs preferentially via oxidative addition. Their calculations also confirmed that Pt$^{2+}-$CH$_3$ can be oxidized to Pt$^{4+}-$CH$_3$ by SO$_3$. Goddard and co-workers[5,6] have studied the same system and have investigated the effects of different ligands on the stability and activity of the catalyst. They showed that C$-$H bond activation may occur via electrophilic substitution or oxidative addition, depending on the ligands on the platinum center. Jones et al.[7] have reported experimental and theoretical results for methane conversion to methanol by a mixture of selenic acid and metallic gold in 96 wt % sulfuric acid. Their studies show that methane undergoes an electrophilic substitution reaction, and that the catalytic cycle involves Au$^+-$Au^{3+} or Au$^{2+}-$Au^{4+} pairs. Methane activation involves the abstraction of a proton by a bisulfate group and is characterized by an activation barrier of 28.1 kcal/mol.

Here we report the results of quantum chemical calculations aimed at identifying critical steps involved in the oxidation of methane to acetic acid catalyzed by Pd^{2+} cation present in concentrated sulfuric acid. These calculations were carried out using density functional theory (DFT). The effects of the solvent, sulfuric acid, were described both explicitly and implicitly. Our objectives were to determine the forms in which Pd^{2+} is stabilized in concentrated sulfuric acid and to calculate the changes in internal energy and free energy for the elementary

(1) Periana, R. A.; Mironov, O.; Taube, D.; Bhalla, G.; Jones, C. J. *Science* **2003**, *301*, 814.
(2) Zerella, M.; Kahros, A.; Bell A. T. *J. Catal.* **2005**, in press.
(3) Gilbert, T. M.; Hristov, I.; Ziegler, T. *Organometallics* **2001**, *20*, 1183.
(4) Hristov, I. H.; Ziegler, T. *Organometallics* **2003**, *22*, 1668.
(5) Kua, J.; Xu, X.; Periana, R. A.; Goddard, W. A. *Organometallics* **2002**, *21*, 511.
(6) Xu, X.; Kua, J.; Periana, R. A.; Goddard, W. A. *Organometallics* **2003**, *22*, 2057.
(7) Jones, C. J.; Taube, D.; Ziatdinov, V. R.; Periana, R. A.; Nielsen, R. J.; Oxgaard, J.; Goddard, W. A. *Angew. Chem., Int. Ed.* **2004**, *43*, 4626.

processes involved in the activation of methane, and those involved in the formation of methyl bisulfate and acetic acid. Activation energies and free energies were also determined for all of the key steps. On the basis of our analysis of the reaction pathway, we suggest that octahedrally coordinated Pd^{4+} species are formed during the course of reaction, and that these species are critical to the formation of methyl bisulfate and acetic acid. The thermodynamics relevant to the stabilization of Pd^{2+} in solution were also examined.

Theory

Electronic energies of reactant, product, and transition states were determined using density functional theory (DFT). The B3LYP functional was used to describe electron exchange and correlation, and the 6-31G* basis set was used to locate optimized ground-state and transition-state structures. The LANL2DZ effective core potential was used to describe the Pd atom. All geometry optimizations were done using the Gaussian 03 software.[8] Molden,[9] a freeware, was used for visualization of the geometries and vibrational frequencies. After a particular molecular structure was optimized to a stationary point (transition state or minimum energy structure), its energy was further refined by a calculation at a higher level of accuracy using the LACV3P**++ basis set as implemented in the Jaguar software.[10] Palladium was treated using effective core potentials within the LACV3P**++ basis set. All stationary points were found on the basis of gas-phase calculations, and then their energy in solution was calculated using the Poisson−Boltzmann continuum (PBC) model which is available with Jaguar. The "growing string method" developed by Peters et al.[11] was used to locate the transition state connecting two minimum energy structures. In this method a minimum energy path connecting the reactant and product is estimated without making an initial guess for the reaction path. The point with highest energy on this reaction path is taken to be the transition state. This point is further converged to the exact saddle point by the transition state finding algorithm implemented in the Gaussian 03 software.[8] All transition states reported here were verified to have only one imaginary frequency. The minimum energy paths and frequencies of all transition states are given in the Supporting Information. Free energies were determined within the rigid-rotor, harmonic-oscillator approximation. Standard free energies were calculated by including translational, rotational, and vibrational partition functions. The Hessian matrix required for vibrational analysis was calculated with the LANL2DZ/6-31G* basis set. Details concerning the calculations of free energies in the liquid-phase are given in the Supporting Information, as well as an assessment of the accuracy of PBC calculations. A discussion of the effect of hydrogen bonding between solvent and the solute on the calculated energies is also given in the Supporting Information. All of the energies reported here are based on the liquid-phase calculations, in which the solvation of dissolved species is described by the PBC model. In reporting the energy change of reactions, the symbol ΔE is used to denote the electronic energy change. The symbol $\Delta G°$ is used to denote the standard change in free energy at 453 K. The standard state for all species present in solution is 1 mol/L. The symbols ΔE_a and ΔG_a refer to the energy of activation and free energy of activation, respectively. The energy (E) reported here includes the interaction between the extended solvent and the solute which is handled implicitly. The zero point energy (ZPE) is not included in E. The ZPE corrected values are given in the Supporting Information. Values of ΔE after ZPE correction change by only ±2.0 kcal/mol.

(8) Frisch, M. J.; et al. *Gaussian 03*, revision C.02; Gaussian, Inc.: Wallingford, CT, 2004.
(9) Schaftenaar, G.; Noordik, J. H. *J. Comput.-Aided Mol. Design* **2000**, *14*, 123.
(10) *Jaguar*, 5.5 ed.; Schrodinger, LLC: Portland, OR, 2003.
(11) Peters, B.; Heyden, A.; Bell, A. T.; Chakraborty, A. *J. Chem. Phys.* **2004**, *120*, 7877.
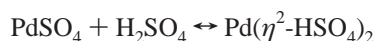
The geometry optimizations in the liquid phase can also be done using the COSMO solvation model implemented in the TURBOMOLE v.5.6 software,[12] but not using other quantum codes. For the cases considered, the change in solvation energy for structures optimized in the gas and liquid phases was negligible. For example, for Pd-(HSO$_4$)$_2$(H$_2$SO$_4$) the solvation energy is −31.25 kcal/mol for the structure optimized in the gas phase and −32.04 kcal/mol for the structure optimized in the liquid phase. These calculations were done with the SV(P) basis set implemented in TURBOMOLE along with the COSMO solvation model.
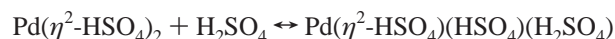
Results and Discussion

Different aspects of the overall reaction pathway are considered in the following subsections. These include solvation of Pd^{2+} cations, activation of methane to form Pd−CH$_3$ bonds, insertion of CO into Pd−CH$_3$ bonds, and formation of final products. The overall reaction pathway and the free energy profile are shown at the end of the Results and Discussion section (Figures 6 and 7). All the reactions mentioned in the text below are listed in Table 1 for easy reference.

Solvation of Palladium. Experimental investigations of methane oxidation to acetic acid catalyzed by Pd^{2+} cations are carried out in concentrated sulfuric acid (typically 96 wt %), and Pd^{2+} is introduced by dissolving either PdSO$_4$ or PdCl$_2$.[1,2] For 70−100 wt % H$_2$SO$_4$, the principal species present in solution are H$_2$SO$_4$, H$_2$O, H$^+$, and HSO$_4^-$. The concentration of ionic species is small, since the pK_a of concentrated sulfuric acid is low (10^{-4}).[13,14]
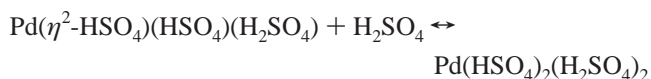
Possible structures for Pd^{2+} solvated in sulfuric acid are shown in Figure 1. PdSO$_4$ can combine with a molecule of H$_2$SO$_4$ to form Pd(η^2-HSO$_4$)$_2$, in which the bisulfate anions are bidentate ligands (viz., η^2 ligation). Further solvent molecules can then add to Pd(η^2-HSO$_4$)$_2$, keeping the Pd^{2+} cation four-coordinated. In sulfuric acid solution, the stable form is palladium bisulfate solvated by one or two solvent molecules. Calculated changes in the internal energy and standard free energy are given below for the solvation reactions. As mentioned earlier, the $\Delta G°$ is determined for 453 K, a representative reaction temperature.

$$PdSO_4 + H_2SO_4 \leftrightarrow Pd(\eta^2\text{-}HSO_4)_2$$

$$\Delta E = -7.0 \text{ kcal/mol}, \quad \Delta G° = -7.2 \text{ kcal/mol} \quad (1)$$

$$Pd(\eta^2\text{-}HSO_4)_2 + H_2SO_4 \leftrightarrow Pd(\eta^2\text{-}HSO_4)(HSO_4)(H_2SO_4)$$

$$\Delta E = -5.2 \text{ kcal/mol}, \quad \Delta G° = -2.5 \text{ kcal/mol} \quad (2)$$

$$Pd(\eta^2\text{-}HSO_4)(HSO_4)(H_2SO_4) + H_2SO_4 \leftrightarrow$$
$$Pd(HSO_4)_2(H_2SO_4)_2$$

$$\Delta E = -4.3 \text{ kcal/mol}, \quad \Delta G° = -6.0 \text{ kcal/mol} \quad (3)$$

All of the Pd^{2+} species exhibit four-fold coordination in a square planar fashion. If additional molecules are brought either above or below the plane, they do not bond with the Pd center. This is true for all of the Pd^{2+} species studied here.

Since 96 wt % H$_2$SO$_4$ contains 16 mol % H$_2$O, it is necessary to consider structures in which H$_2$O acts as a ligand. Two

(12) Treutler, O.; Ahlrichs, R. *J. Chem. Phys.* **1995**, *102*, 346.
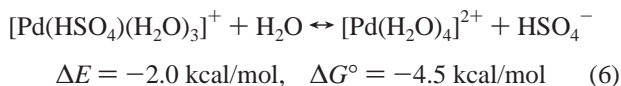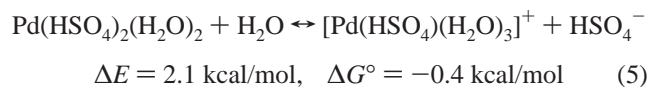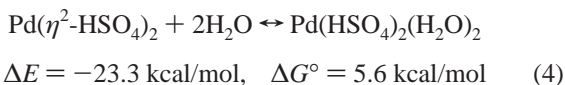(13) Kazansky, V. B. *Catal. Today* **2002**, *73*, 127.
(14) Kazansky, V.; Solkan, V. *Phys. Chem. Chem. Phys.* **2003**, *5*, 31.

Table 1. Summary of Reactions[a]

| eq no.	reaction	ΔE^a	ΔG^a
	Palladium Solvation		
1	$PdSO_4 + H_2SO_4 \leftrightarrow Pd(\eta^2\text{-}HSO_4)_2$	−7.0	−7.2
2	$Pd(\eta^2\text{-}HSO_4)_2 + H_2SO_4 \leftrightarrow Pd(\eta^2\text{-}HSO_4)(HSO_4)(H_2SO_4)$	−5.2	−2.5
3	$Pd(\eta^2\text{-}HSO_4)(HSO_4)(H_2SO_4) + H_2SO_4 \leftrightarrow Pd(HSO_4)_2(H_2SO_4)_2$	−4.3	−6.0
4	$Pd(\eta^2\text{-}HSO_4)_2 + 2H_2O \leftrightarrow Pd(HSO_4)_2(H_2O)_2$	−23.3	+5.6
5	$Pd(HSO_4)_2(H_2O)_2 + H_2O \leftrightarrow [Pd(HSO_4)(H_2O)_3]^+ + HSO_4^-$	−2.1	−0.4
6	$[Pd(HSO_4)(H_2O)_3]^+ + H_2O \leftrightarrow [Pd(H_2O)_4]^{2+} + HSO_4^-$	−2.0	−4.5
	Methane Activation		
7	$Pd(\eta^2\text{-}HSO_4)(HSO_4)(H_2SO_4) + CH_4 \rightarrow Pd(\eta^2\text{-}HSO_4)(HSO_4)(CH_3)(H)(H_2SO_4)$	+30.4	+44.0
8	$Pd(\eta^2\text{-}HSO_4)_2 + CH_4 \rightarrow Pd(\eta^2\text{-}HSO_4)(CH_3)(H_2SO_4)$	+2.9	+13.7
9a	$Pd(\eta^2\text{-}HSO_4)(HSO_4)(H_2SO_4) + CH_4 \rightarrow Pd(HSO_4)(CH_3)(H_2SO_4)_2$	−4.6	+8.6
9b	$Pd(\eta^2\text{-}HSO_4)(HSO_4)(H_2SO_4) + CH_4 \rightarrow Pd(HSO_4)(CH_3)(H_2SO_4)_2$	+5.5	+18.3
10	$Pd(HSO_4)_2(H_2SO_4)_2 + CH_4 \rightarrow Pd(HSO_4)_2(H_2SO_4)(CH_4) + H_2SO_4$	+15.3	+28.8
	CO Insertion		
11	$Pd(\eta^2\text{-}HSO_4)(HSO_4)(H_2SO_4) + CO \leftrightarrow Pd(\eta^2\text{-}HSO_4)(HSO_4)(CO) + H_2SO_4$	−13.1	+2.1
12	$Pd(HSO_4)_2 (H_2SO_4)_2 + CO \leftrightarrow Pd(HSO_4)_2(H_2SO_4)(CO) + H_2SO_4$	−8.9	+6.0
13	$Pd(HSO_4)(CH_3)(H_2SO_4)_2 + CO \leftrightarrow Pd(HSO_4)(CH_3)(CO)(H_2SO_4) + H_2SO_4$	−24.5	+14.4
14	$Pd(HSO_4)(CH_3)(CO)(H_2SO_4) + H_2SO_4 \rightarrow Pd(HSO_4)(CH_3CO)(H_2SO_4)_2$	+8.0	+14.0
	Product Formation		
15	$Pd(HSO_4)(CH_3)(H_2SO_4)_2 \rightarrow Pd(H_2SO_4)_2 + CH_3HSO_4$	+35.5	+17.0
16	$Pd(HSO_4)(CH_3CO)(H_2SO_4)_2 \rightarrow Pd(H_2SO_4)_2 + CH_3COHSO_4$	+28.7	+7.7
17	$Pd(HSO_4)(CH_3)(H_2SO_4)_2 + H_2O \rightarrow Pd(HSO_4)(H)(H_2SO_4)_2 + CH_3OH$	+21.3	+23.4
18	$Pd(HSO_4)_2(H_2SO_4)_2 + H_2SO_4 + {}^1\!/_2O_2 \rightarrow Pd(\eta^2\text{-}HSO_4)(HSO_4)_3(H_2SO_4) + H_2O$	+25.3	+27.0
19	$Pd(HSO_4)(CH_3)(H_2SO_4)_2 + H_2SO_4 + {}^1\!/_2O_2 \rightarrow Pd(\eta^2\text{-}HSO_4)(HSO_4)_2(CH_3) (H_2SO_4) + H_2O$	−11.8	−8.6
20	$Pd(HSO_4)(CH_3CO)(H_2SO_4)_2 + H_2SO_4 + {}^1\!/_2O_2 \rightarrow Pd(\eta^2\text{-}HSO_4)(HSO_4)_2(CH_3CO)(H_2SO_4)_2 + H_2O$	−14.3	−14.0
21	$H_2SO_4 \rightarrow H_2O + SO_2 + {}^1\!/_2O_2$	+19.5	−4.7
22	$Pd(\eta^2\text{-}HSO_4)(HSO_4)_2(CH_3)(H_2SO_4) \rightarrow Pd(\eta^2\text{-}HSO_4)(HSO_4)(H_2SO_4) + CH_3HSO_4$	−38.1	−53.7
23	$Pd(\eta^2\text{-}HSO_4)(HSO_4)_2(CH_3CO)(H_2SO_4) \rightarrow Pd(\eta^2\text{-}HSO_4)(HSO_4)(H_2SO_4) + CH_3COHSO_4$	−19.2	−35.6
24	$Pd(\eta^2\text{-}HSO_4)(HSO_4)(H_2SO_4) + CO + H_2O \rightarrow Pd(H_2SO_4)_2 + CO_2 + H_2SO_4$	−3.6	−11.5
25	$Pd(HSO_4)_2(H_2SO_4)_2 + CO + H_2O \rightarrow Pd(H_2SO_4)_2 + CO_2 + 2H_2SO_4$	−2.9	−31.2
26	$CH_3HSO_4 + H_2SO_4 \rightarrow CO + H_2O + 2H_2SO_3$	−39.0	−70.5
27	$Pd(H_2SO_4)_2 + H_2SO_4 \rightarrow Pd(\eta^2\text{-}HSO_4)_2 + SO_2 + 2H_2O$	−48.2	−76.3
28	$Pd(H_2SO_4)_2 + {}^1\!/_2O_2 \rightarrow Pd(\eta^2\text{-}HSO_4)_2 + H_2O$	−67.7	−71.6

[a] The thermochemistry of all reactions mentioned in the text is summarized here. The energies are in kcal/mol. ΔE refers to energy (kcal/mol) without zero-point corrections, but including the solvation corrections. ΔG refers to the free energy (kcal/mol) at 453 K, which includes contributions from the vibrational, rotational, and translational degrees of freedom. All energies and free energies are in kcal/mol.

alternatives are shown in Figure 1 (structures **E** and **F**). Energy changes for the processes in which water replaces bisulfate anions or sulfuric acid are given below.

$$Pd(\eta^2\text{-}HSO_4)_2 + 2H_2O \leftrightarrow Pd(HSO_4)_2(H_2O)_2$$

$$\Delta E = -23.3 \text{ kcal/mol}, \quad \Delta G^\circ = 5.6 \text{ kcal/mol} \quad (4)$$

$$Pd(HSO_4)_2(H_2O)_2 + H_2O \leftrightarrow [Pd(HSO_4)(H_2O)_3]^+ + HSO_4^-$$

$$\Delta E = 2.1 \text{ kcal/mol}, \quad \Delta G^\circ = -0.4 \text{ kcal/mol} \quad (5)$$

$$[Pd(HSO_4)(H_2O)_3]^+ + H_2O \leftrightarrow [Pd(H_2O)_4]^{2+} + HSO_4^-$$

$$\Delta E = -2.0 \text{ kcal/mol}, \quad \Delta G^\circ = -4.5 \text{ kcal/mol} \quad (6)$$

Comparison of the values of ΔG° for eqs 1−3 and 4−6 shows that the displacement of H_2SO_4 or HSO_4 as ligands by H_2O is not favored thermodynamically in concentrated sulfuric acid. Estimates of the relative fractions of various Pd^{2+} species are summarized in Table 2 for solutions containing 70−100 wt % H_2SO_4. The results reported in this table are based on the experimental values[15] for the concentrations of H_2O, H_2SO_4, and HSO_4^- and the values of ΔG° reported here (see eqs 1−6). Table 2 shows that the dominant form of dissolved Pd^{2+} is predicted to be $Pd(HSO_4)_2(H_2SO_4)_2$, whereas $Pd(\eta^2\text{-}HSO_4)$-$(HSO_4)(H_2SO_4)$ and $Pd(\eta^2\text{-}HSO_4)_2$ are present in much smaller concentrations.

Work by Kazansky and co-workers[13,14] shows that concentrated sulfuric acid (∼96 wt %) contains a lower concentration of protons than a dilute solution of H_2SO_4 in water. The reason

(15) Robertson, E. B.; Dunford, H. B. *J. Am. Chem. Soc.* **1964**, *86*, 5080.
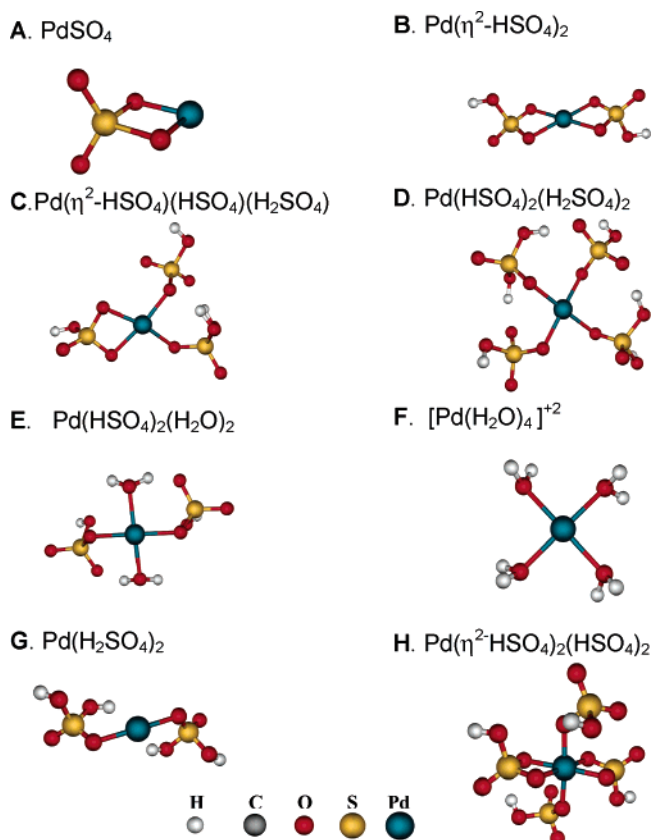
Figure 1. Structures of Pd solvated in sulfuric acid. Structures **A**−**F** are Pd^{2+} species. Structure **G** is an example of a Pd^0 species, and structure **H** is an example of a Pd^{4+} species.

Table 2. Relative Fractions of Pd^{2+} Species[a]

| wt % H$_2$SO$_4$	mol % H$_2$O	[Pd(H$_2$O)$_4$]$^{2+}$	Pd(η^2-HSO$_4$)$_2$	Pd(η^2-HSO$_4$)(HSO$_4$)(H$_2$SO$_4$)	Pd(HSO$_4$)$_2$(H$_2$SO$_4$)$_2$
74.6	47.6	0.2547	0.6231	0.0336	0.0885
79.7	41.4	0.0096	0.0590	0.0329	0.8985
85.5	34.7	0.0001	0.0016	0.0056	0.9927
89.8	28.5	0	0.0005	0.0031	0.9964
90.7	27.0	0	0.0004	0.0028	0.9968
93.6	21.9	0	0.0002	0.0021	0.9977
95.1	18.6	0	0.0002	0.0018	0.9980
96.7	14.3	0	0.0001	0.0016	0.9983
97.5	11.7	0	0.0001	0.0015	0.9983
98.0	9.9	0	0.0001	0.0015	0.9984
99.0	5.3	0	0.0001	0.0013	0.9986

[a] Relative fractions of Pd species are given in the last four columns. Other Pd species are present in negligible concentrations at these conditions. The second column gives the mol % of water vs the wt % of sulfuric acid. All equilibrium constants used for these calculations are based on the quantum chemical calculations reported in this work and are evaluated at a temperature of 453 K. Experimentally determined equilibrium constants at 298 K for the water-containing species (e.g., [Pd(H$_2$O)$_4$]$^{2+}$) are available in the literature[16,17] but are not used here.

for this is that H$_2$SO$_4$ is much less effective at solvating protons than is H$_2$O. As a consequence, the dissociation constant of H$_2$-SO$_4$ is only 10^{-4} in anhydrous H$_2$SO$_4$. Consistent with this, our calculations also show that dissociation of H$_2$SO$_4$ to HSO$_4^-$ and H$_3$SO$_4^+$ is energetically uphill ($\Delta E = +19.8$ kcal/mol, $\Delta G = +21.2$ kcal/mol). We also examined the possibility that the reactants and products we have considered are protonated. For example, protonation of the reactant in eq 9a, Pd(η^2-HSO$_4$)-(HSO$_4$)(H$_2$SO$_4$), requires an energy of $+14.6$ kcal/mol to form [Pd(η^2-HSO$_4$)(H$_2$SO$_4$)$_2$]$^+$. Similarly, protonation of the product of Pd(HSO$_4$)(CH$_3$)(H$_2$SO$_4$) to form [PdCH$_3$(H$_2$SO$_4$)$_3$]$^+$ requires an energy of $+18.8$ kcal/mol. These values are calculated assuming one molecule of H$_2$SO$_4$ reacts with the Pd species to form the protonated product and HSO$_4^-$. Thus we conclude that protonated species are unlikely to be found in our reaction system.

Methane Activation. The addition of methane to structures **B**, **C**, and **D** (Figure 1) leads in all cases to the formation of Pd$-$CH$_3$ bonds. Only those reactions in which CH$_3$ is attached to Pd and a proton is attached to the oxygen atom of an HSO$_4^-$ group were found to be thermodynamically favorable. As exemplified by eq 7, oxidative addition of CH$_4$ to Pd^{2+} to produce an octahedrally coordinated product is highly unfavorable thermodynamically.

$$Pd(\eta^2\text{-HSO}_4)(HSO_4)(H_2SO_4) + CH_4 \rightarrow$$
$$Pd(\eta^2\text{-HSO}_4)(HSO_4)(CH_3)(H)(H_2SO_4)$$
$$\Delta E = 30.4 \text{ kcal/mol}, \quad \Delta G° = 44.0 \text{ kcal/mol} \quad (7)$$

$$Pd(\eta^2\text{-HSO}_4)_2 + CH_4 \rightarrow Pd(\eta^2\text{-HSO}_4)(CH_3)(H_2SO_4)$$
$$\Delta E = 2.9 \text{ kcal/mol}, \quad \Delta G° = 13.7 \text{ kcal/mol} \quad (8)$$
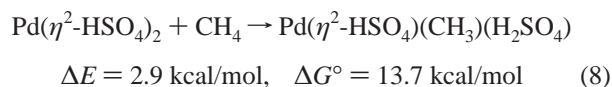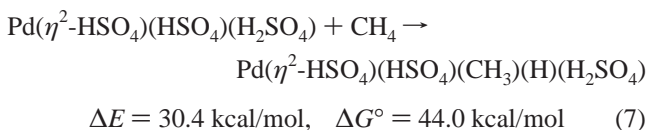
By contrast, eq 8, which involves the transfer of a proton from methane to a bisulfate ligand, is more favorable. The structures of the reactant, transition, and product states for this reaction are illustrated in Figure 2. The activation barrier for eq 8 is $\Delta E_a = 27.8$ kcal/mol, and the free energy of activation is $\Delta G_a = 38.1$ kcal/mol.
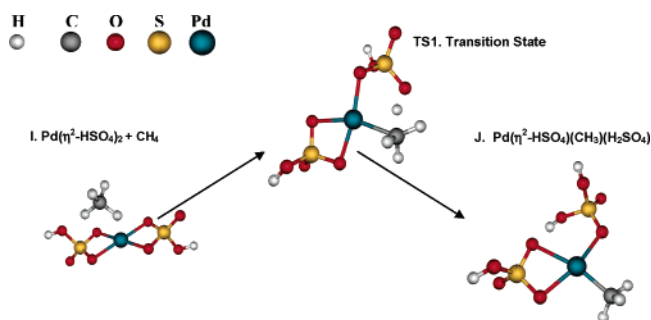
Figure 2. Activation of methane over Pd(η^2-HSO$_4$)$_2$ to form a Pd$-$CH$_3$ bond.
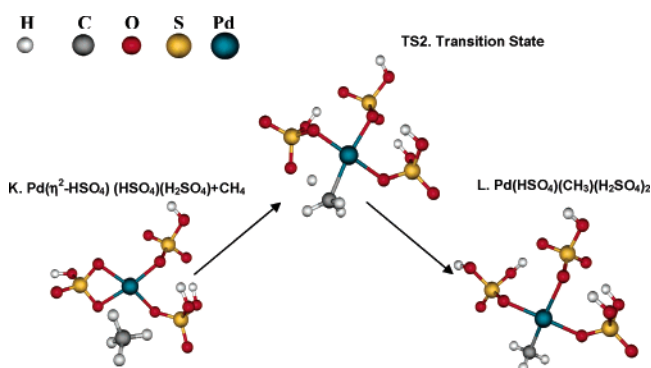
Figure 3. Activation of methane over Pd(η^2-HSO$_4$)(HSO$_4$)(H$_2$SO$_4$), pathway 1. CH$_4$ is added across the bidentate bond, converting the bidentate HSO$_4$ to an H$_2$SO$_4$ ligand. (Eq 9a: Pd(η^2-HSO$_4$)(HSO$_4$)(H$_2$SO$_4$) + CH$_4$ $\rightarrow$ Pd(HSO$_4$)(CH$_3$)(H$_2$SO$_4$)$_2$; $\Delta E = -4.6$ kcal/mol, $\Delta G° = +8.6$ kcal/mol.)
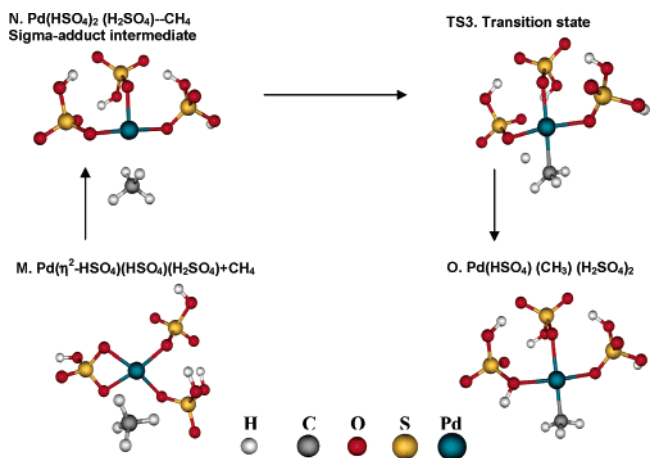
Figure 4. Methane activation which involves a σ-adduct intermediate. The species at the bottom right (structure **O**) will undergo further rearrangement to structure **L** of Figure 3. (Eq 9b: Pd(η^2-HSO$_4$)(HSO$_4$)(H$_2$SO$_4$) + CH$_4$ $\rightarrow$ Pd(HSO$_4$)(CH$_3$)(H$_2$SO$_4$)$_2$; $\Delta E = 5.5$ kcal/mol, $\Delta G° = +18.3$ kcal/mol.)

Methane can be also be activated by Pd(η^2-HSO$_4$)(HSO$_4$)(H$_2$-SO$_4$), as shown in eq 9. As shown in Figures 3 and 4, there are

$$Pd(\eta^2\text{-HSO}_4)(HSO_4)(H_2SO_4) + CH_4 \rightarrow$$
$$Pd(HSO_4)(CH_3)(H_2SO_4)_2 \quad (9)$$
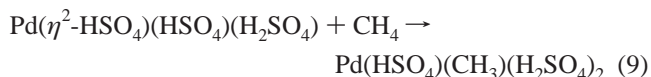
two pathways by which this reaction can proceed. These correspond to eqs 9a and 9b defined in the captions for Figures 3 and 4. Neither the transition states nor the final states for these reactions are equivalent. As shown in Figure 3, the first pathway, eq 9a, involves the transfer of a proton from CH$_4$ to an O atom of the η^2-HSO$_4$ ligand in such a way that, at the end of the

reaction, the proton is bound to one of the two O atoms that is not bonded to Pd. In this instance, $\Delta E = -4.6$ kcal/mol and $\Delta G° = 8.6$ kcal/mol, and the activation energy and free energy are $\Delta E_a = 27.9$ kcal/mol and $\Delta G_a = 41.5$ kcal/mol. Figure 4 shows that, in the second case, eq 9b, CH_4 adsorbs in the form of a σ-adduct by replacing one of the Pd–O bonds of the bidentate ligand ($\Delta E = 12.5$ kcal/mol, $\Delta G° = 25.3$ kcal/mol). A proton from CH_4 is then transferred to one of the oxygens bound to Pd (see Figure 4; $\Delta E = -7.0$ kcal/mol, $\Delta G° = -7.0$ kcal/mol). The activation barrier for this proton-transfer step is $\Delta E_a = 23.2$ kcal/mol, and the free energy of activation is $\Delta G_a = 24.5$ kcal/mol. We note that the proton transferred from methane ends up in slightly different positions in these two pathways. The end product of eq 9b can rearrange to the low-energy form (structure **L**, Figure 3), which is the end product of eq 9a ($\Delta E = -10.1$ kcal/mol, $\Delta G° = -9.8$ kcal/mol).

The addition of CH_4 to $Pd(HSO_4)_2(H_2SO_4)_2$, structure **D** in Figure 1, occurs via a path similar to that shown in Figure 4. As illustrated by eq 10, the reaction begins with the replacement of one of the H_2SO_4 ligands by a CH_4 molecule, which then forms a σ-adduct with the Pd cation, a structure which is identical to **N** in Figure 4. The subsequent steps in the reaction pathway are identical to those shown in Figure 4.
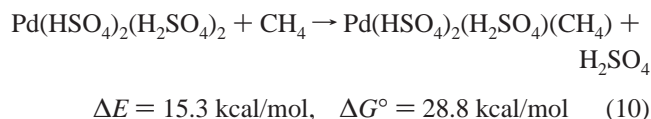
$$Pd(HSO_4)_2(H_2SO_4)_2 + CH_4 \rightarrow Pd(HSO_4)_2(H_2SO_4)(CH_4) + H_2SO_4$$

$$\Delta E = 15.3 \text{ kcal/mol}, \quad \Delta G° = 28.8 \text{ kcal/mol} \quad (10)$$

Table 2 indicates that, in 96 wt % sulfuric acid, Pd^{2+} cations are present primarily as $Pd(HSO_4)_2(H_2SO_4)_2$ and to a lesser extent as $Pd(\eta^2\text{-}HSO_4)(HSO_4)(H_2SO_4)$. Nevertheless, the results presented above suggest that the primary pathway for methane activation is via eq 9a, which involves $Pd(\eta^2\text{-}HSO_4)(HSO_4)(H_2SO_4)$, rather than via eq 10, which involves $Pd(HSO_4)_2(H_2SO_4)_2$. The reason for excluding eq 10, and likewise eq 9b, is the unfavorable thermodynamics for forming the σ-adduct of CH_4 with either $Pd(HSO_4)_2(H_2SO_4)_2$ or $Pd(\eta^2\text{-}HSO_4)(HSO_4)(H_2SO_4)$. Moreover, the overall barrier for methane activation via eqs 10 and 9b is 53.3 kcal/mol, whereas eq 9a has a barrier of 41.5 kcal/mol. This difference of 11.8 kcal/mol compensates for the fact that the free energy of $Pd(HSO_4)_2(H_2SO_4)_2$ is lower than that of $Pd(\eta^2\text{-}HSO_4)(HSO_4)(H_2SO_4)$ by 6.2 kcal/mol (see eq 3). It is noted further that methane activation via eq 8 is projected to occur at roughly the same rate as that via eq 9a. While the concentration of $Pd(\eta^2\text{-}HSO_4)_2$ is predicted to be lower than that of $Pd(\eta^2\text{-}HSO_4)(HSO_4)(H_2SO_4)$ (see Table 2, and eq 2), the free energy of activation via eq 8, in which CH_4 reacts with $Pd(\eta^2\text{-}HSO_4)_2$, is lower than that for eq 9a by 3.4 kcal/mol. This difference of 3.4 kcal/mol compensates for the fact that the free energy of $Pd(\eta^2\text{-}HSO_4)_2$ is lower than that of $Pd(\eta^2\text{-}HSO_4)(HSO_4)(H_2SO_4)$ by 2.5 kcal/mol.
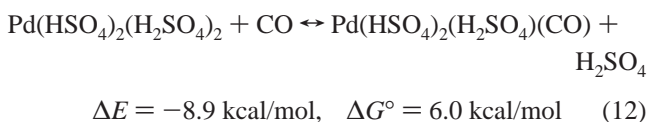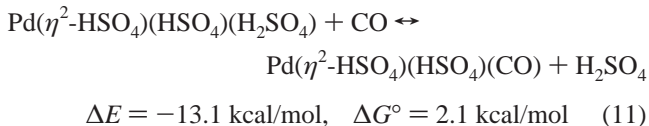
Insertion of CO. Periana et al.[1] have suggested that the carbon atom associated with the carboxylate group of acetic acid is formed by the insertion of CO into the Pd–CH_3 complex formed upon the activation of CH_4. More recently, Zerella and Bell[2] have established that CO is formed via the oxidation of methyl bisulfate, an intermediate formed during the oxidation of CH_4. Both the source of CO and its role in forming the carboxylate group of acetic acid were confirmed in experiments using ^{13}C-labeled methyl bisulfate (produced by reaction of
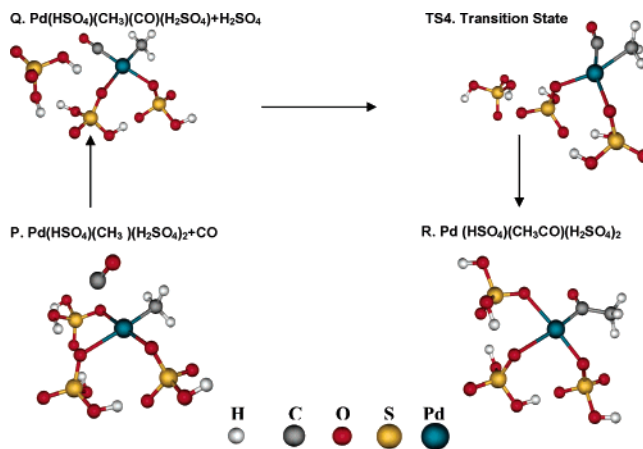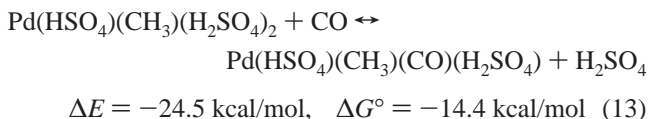
Figure 5. Illustration of the processes involved in the formation of acyl species.

$^{13}CH_3OH$ and H_2SO_4) and ^{13}CO. These experiments confirmed that ^{13}C is only present as $CH_3^{13}COOH$. Consistent with these findings, we have determined that the oxidation of CH_3HSO_4 by either H_2SO_4 or O_2 to form CO and associated products is highly favorable.
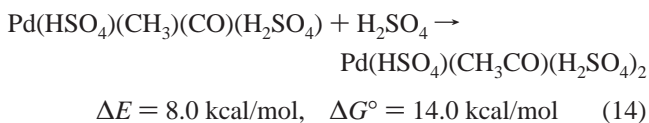
Calculations were made in the course of the present study to identify the pathways by which CO interacts with the Pd–CH_3 complexes. These calculations show that CO can displace a molecule of H_2SO_4 to form $Pd(\eta^2\text{-}HSO_4)(HSO_4)(CO)$, even when there is no CH_3 ligand, as in eqs 11 and 12.

$$Pd(\eta^2\text{-}HSO_4)(HSO_4)(H_2SO_4) + CO \leftrightarrow$$
$$Pd(\eta^2\text{-}HSO_4)(HSO_4)(CO) + H_2SO_4$$

$$\Delta E = -13.1 \text{ kcal/mol}, \quad \Delta G° = 2.1 \text{ kcal/mol} \quad (11)$$

$$Pd(HSO_4)_2(H_2SO_4)_2 + CO \leftrightarrow Pd(HSO_4)_2(H_2SO_4)(CO) + H_2SO_4$$

$$\Delta E = -8.9 \text{ kcal/mol}, \quad \Delta G° = 6.0 \text{ kcal/mol} \quad (12)$$

The activation energy and the free energy of activation are $\Delta E_a = 8.2$ kcal/mol and $\Delta G_a = 15.0$ kcal/mol for eq 11. In the case of the CH_3-containing species, $Pd(HSO_4)(CH_3)(H_2SO_4)_2$, $\Delta E = -24.5$ kcal/mol and $\Delta G° = -14.4$ kcal/mol, and this reaction (eq 13) proceeds without an activation barrier.

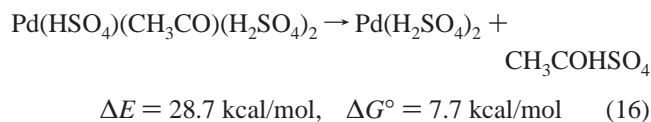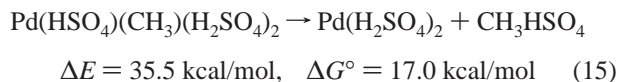$$Pd(HSO_4)(CH_3)(H_2SO_4)_2 + CO \leftrightarrow$$
$$Pd(HSO_4)(CH_3)(CO)(H_2SO_4) + H_2SO_4$$

$$\Delta E = -24.5 \text{ kcal/mol}, \quad \Delta G° = -14.4 \text{ kcal/mol} \quad (13)$$

Adsorbed CO can then insert into the Pd–CH_3 bond to form an acyl species (see Figure 5).

$$Pd(HSO_4)(CH_3)(CO)(H_2SO_4) + H_2SO_4 \rightarrow$$
$$Pd(HSO_4)(CH_3CO)(H_2SO_4)_2$$

$$\Delta E = 8.0 \text{ kcal/mol}, \quad \Delta G° = 14.0 \text{ kcal/mol} \quad (14)$$
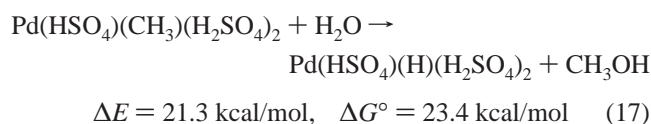
The activation energy and the free energy of activation for eq 14 are $\Delta E_a = 15.1$ kcal/mol and $\Delta G_a = 14.7$ kcal/mol. We have also considered the addition of CO to Pd catalyst first, followed by the activation of methane. The barrier for activation of CH_4 by $Pd(\eta^2\text{-}HSO_4)(HSO_4)(CO)$ has a value of 27 kcal/mol, which is similar to that for eq 8.

Formation of CH₃HSO₄ and CH₃COOH. Periana et al.[1] and Zerella et al.[18] have proposed that methyl bisulfate and the mixed anhydride of acetic and sulfuric acid, CH₃COHSO₄, are formed via intramolecular processes, eqs 15 and 16, below. With the amounts of water present in 96 wt % H₂SO₄, the mixed anhydride hydrolyzes to acetic acid and sulfuric acid, whereas methyl bisulfate is stable to hydrolysis. Both sets of authors have proposed that zero-valent Pd atoms are formed during the release of products, e.g., eqs 15 and 16.

$$Pd(HSO_4)(CH_3)(H_2SO_4)_2 \rightarrow Pd(H_2SO_4)_2 + CH_3HSO_4$$

$$\Delta E = 35.5 \text{ kcal/mol}, \quad \Delta G° = 17.0 \text{ kcal/mol} \quad (15)$$

$$Pd(HSO_4)(CH_3CO)(H_2SO_4)_2 \rightarrow Pd(H_2SO_4)_2 + CH_3COHSO_4$$

$$\Delta E = 28.7 \text{ kcal/mol}, \quad \Delta G° = 7.7 \text{ kcal/mol} \quad (16)$$

While the present calculations show that the thermodynamics for these processes are moderately unfavorable, the formation of Pd-black formation (viz., Pd → ¹/₆Pd₆, $\Delta E = -32.6$ kcal/mol, $\Delta G° = -23.4$ kcal/mol) makes these reactions thermodynamically favorable. Nevertheless, eqs 15 and 16 are unlikely to proceed, since the activation barriers for these reactions are very high, and it was not possible to identify a pathway by which these reactions might proceed with a reasonable barrier. For example, in the case of eq 15 we have estimated[19] the activation barrier to be 49 kcal/mol.

Since 96 wt % sulfuric acid contains ~16 mol % water, it is reasonable to consider the hydrolysis of Pd−(CH₃)- and Pd−(CH₃CO)-containing species as processes by which methanol and acetic acid might form, respectively. The methanol released by the first of these reactions would react immediately with H₂SO₄ to form methyl bisulfate. An example of such a reaction, for which palladium hydride is one of the products, is given by eq 17. It is apparent that the Gibbs free energy change for this reaction is relatively high; therefore, this process seems unlikely to occur.
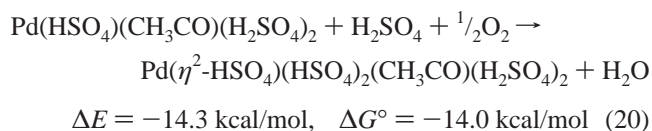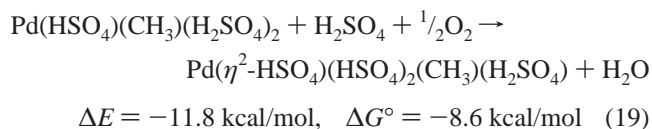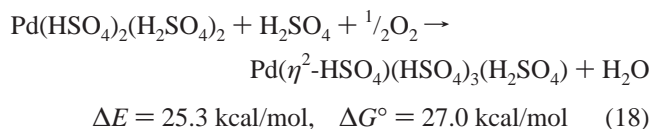
$$Pd(HSO_4)(CH_3)(H_2SO_4)_2 + H_2O \rightarrow Pd(HSO_4)(H)(H_2SO_4)_2 + CH_3OH$$

$$\Delta E = 21.3 \text{ kcal/mol}, \quad \Delta G° = 23.4 \text{ kcal/mol} \quad (17)$$

The hydrolysis of Pd−CH₃CO to form acetic acid is thermodynamically favorable, but the activation barrier was estimated[19] to be around 80 kcal/mol. Consequently, this process is unlikely to be the principal route to acetic acid.

As an alternative to eqs 15−17, we examined the possibility that Pd²⁺ species undergo oxidation to Pd⁴⁺ species, and that methyl bisulfate and the mixed anhydride of acetic acid and sulfuric acid are then produced via intramolecular processes from these Pd⁴⁺ species. These processes are similar to those examined by Xu et al.[20] and Hristov and Ziegler[4] for the

case of methane oxidation to methanol catalyzed by Pt²⁺ in sulfuric acid. While the oxidation of Pd²⁺ to Pd⁴⁺ does not have many precedents, stable octahedral Pd⁴⁺ complexes have been reported, some of which contain methyl and ethyl ligands.[21−23]

The oxidation of Pd²⁺ to Pd⁴⁺ can be envisioned to occur via reaction with H₂SO₄ and O₂ (eqs 18−20). Note that the octahedral Pd⁴⁺ species on the right-hand side of these equations always has a bidentate η^2-HSO₄ ligand. Replacement of one η^2-HSO₄ ligand by the combination of an HSO₄ ligand and an H₂SO₄ ligand is not favored, because the presence of two ligands instead of one leads to crowding around the Pd atom.

$$Pd(HSO_4)_2(H_2SO_4)_2 + H_2SO_4 + {}^1\!/_2O_2 \rightarrow Pd(\eta^2\text{-}HSO_4)(HSO_4)_3(H_2SO_4) + H_2O$$

$$\Delta E = 25.3 \text{ kcal/mol}, \quad \Delta G° = 27.0 \text{ kcal/mol} \quad (18)$$

$$Pd(HSO_4)(CH_3)(H_2SO_4)_2 + H_2SO_4 + {}^1\!/_2O_2 \rightarrow Pd(\eta^2\text{-}HSO_4)(HSO_4)_2(CH_3)(H_2SO_4) + H_2O$$

$$\Delta E = -11.8 \text{ kcal/mol}, \quad \Delta G° = -8.6 \text{ kcal/mol} \quad (19)$$

$$Pd(HSO_4)(CH_3CO)(H_2SO_4)_2 + H_2SO_4 + {}^1\!/_2O_2 \rightarrow Pd(\eta^2\text{-}HSO_4)(HSO_4)_2(CH_3CO)(H_2SO_4)_2 + H_2O$$

$$\Delta E = -14.3 \text{ kcal/mol}, \quad \Delta G° = -14.0 \text{ kcal/mol} \quad (20)$$

It is evident that the thermodynamics of oxidizing Pd²⁺ to Pd⁴⁺ are not favorable for eq 18. However, when CH₃ or CH₃-CO is part of the Pd²⁺ complex, the oxidation of Pd²⁺ to Pd⁴⁺ is readily accomplished. This is a direct result of the stabilization of Pd⁴⁺ by the alkyl or acyl ligand. While eqs 18−20 are written assuming an external source of O₂, the oxidation of Pd²⁺ to Pd⁴⁺ can also proceed with sulfuric acid acting as the oxidizing agent. The free energy changes for such processes are obtained by adding the value of $\Delta G°$ for eq 21 to that for eq 18, 19, or 20.

The elementary steps which lead to the oxidation of Pd²⁺ to Pd⁴⁺ may involve participation of two or more sulfuric acid molecules. We did not attempt to find transition states for these reactions because these calculations require a very large expenditure of computing resources. The ability of H₂SO₄ or H₂SO₄/O₂ to oxidize Pd metal to Pd²⁺ has been demonstrated in our laboratory,[2] and hence it is reasonable to expect that the oxidation of Pd²⁺ to Pd⁴⁺ in sulfuric acid would follow a mechanism similar to that proposed for the oxidation of Pt²⁺ to Pt⁴⁺ under similar conditions.[4,6] The thermodynamics calculations given in eqs 19 and 20 show that the oxidation of Pd-
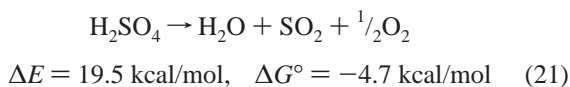
(16) Shi, T. S.; Elding, L. I. *Acta Chem. Scand.* **1998**, *52*, 897.
(17) Rudakov, E. S.; Yaroshenko, A. P.; Rudakova, R. I.; Zamashchikov, V. V. *Ukr. Khim. Zh.* **1984**, *50*, 680.
(18) Zerella, M.; Mukhopadhyay, S.; Bell, A. T. *Chem. Commun.* **2004**, 1948.
(19) The growing string method produces a minimum energy path, and the highest energy point on this path is the first guess for transition state. In most cases we were able to converge accurately to the saddle point starting from this initial guess. In a few cases, where we could not converge to a saddle point, the initial guess itself is taken as the transition state.

(20) Xu, X.; Fu, G.; Goddard, W. A.; Periana, R. A. Selective oxidation of CH₄ to CH₃OH using the Catalytica (bpym)PtCl₂ catalyst: a theoretical study. In *Natural Gas Conversion VII*, Proceedings of the 7th Natural Gas Conversion Symposium, June 6−10, 2004, Dalian, China; Bao, X., Xu, Y., Eds.; Elsevier: Amsterdam, 2004; Vol. 147, p 499.
(21) Campora, J.; Palma, P.; del Rio, D.; Carmona, E.; Graiff, C.; Tiripicchio, A. *Organometallics* **2003**, *22*, 3345.
(22) Canty, A. J.; Denney, M. C.; Patel, J.; Sun, H. L.; Skelton, B. W.; White, A. H. *J. Organomet. Chem.* **2004**, *689*, 672.
(23) Yamamoto, Y.; Kuwabara, S.; Matsuo, S.; Ohno, T.; Nishiyama, H.; Itoh, K. *Organometallics* **2004**, *23*, 3898.
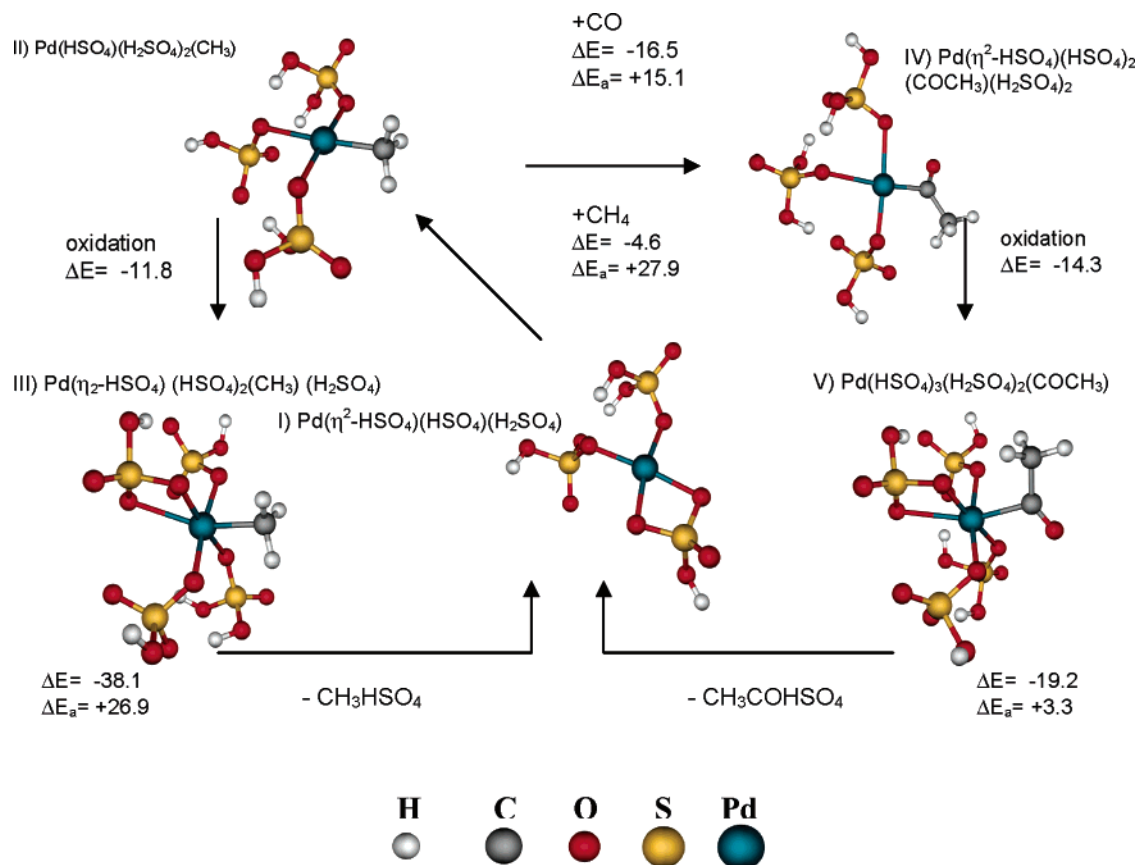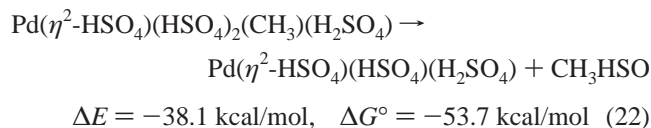
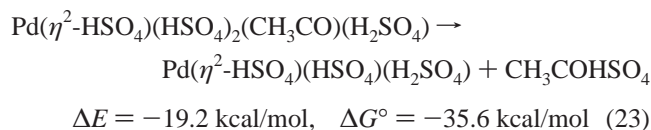**Figure 6.** Overall reaction pathway for the formation of CH_3HSO_4 and CH_3COHSO_4.

$(HSO_4)(CH_3)(H_2SO_4)_2$ and $Pd(HSO_4)(CH_3CO)(H_2SO_4)_2$ is thermodynamically favored.

$$H_2SO_4 \rightarrow H_2O + SO_2 + \tfrac{1}{2}O_2$$

$$\Delta E = 19.5 \text{ kcal/mol}, \quad \Delta G° = -4.7 \text{ kcal/mol} \quad (21)$$

The release of products from Pd^{4+} complexes is thermodynamically feasible and does not involve high activation barriers. Equation 22 illustrates how CH_3HSO_4 is formed.

$$Pd(\eta^2\text{-}HSO_4)(HSO_4)_2(CH_3)(H_2SO_4) \rightarrow$$
$$Pd(\eta^2\text{-}HSO_4)(HSO_4)(H_2SO_4) + CH_3HSO$$

$$\Delta E = -38.1 \text{ kcal/mol}, \quad \Delta G° = -53.7 \text{ kcal/mol} \quad (22)$$

The activation energy and free energy of activation for eq 22 are $\Delta E_a = 26.9$ kcal/mol and $\Delta G_a = 27.5$ kcal/mol. A similar reaction for the formation of CH_3COHSO_4 is represented by eq 23.

$$Pd(\eta^2\text{-}HSO_4)(HSO_4)_2(CH_3CO)(H_2SO_4) \rightarrow$$
$$Pd(\eta^2\text{-}HSO_4)(HSO_4)(H_2SO_4) + CH_3COHSO_4$$

$$\Delta E = -19.2 \text{ kcal/mol}, \quad \Delta G° = -35.6 \text{ kcal/mol} \quad (23)$$
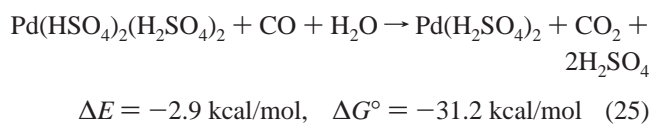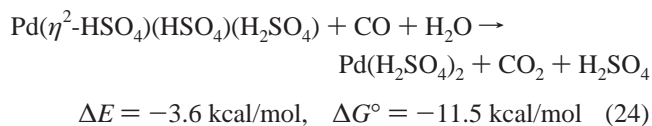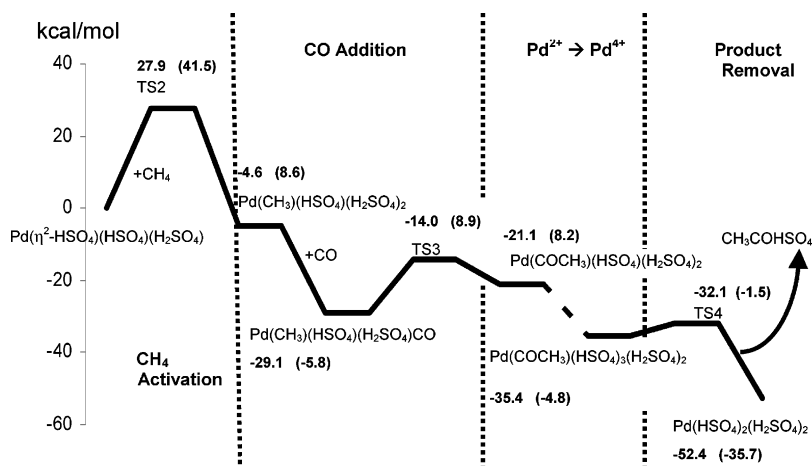
The activation energy and free energy of activation for eq 23 are estimated[24] to be $\Delta E_a = 3.3$ kcal/mol and $\Delta G_a = 3.3$ kcal/mol.

The overall catalytic cycle is shown in Figure 6, and the free energy change along a representative pathway is given in Figure 7. The catalytic cycle shown in Figure 6 closely resembles that

proposed by Zerella and Bell on the basis of experimental studies.[2] These authors demonstrated that the source of CO required for the formation of the carboxylate group in acetic acid is oxidation of CH_3HSO_4, the primary byproduct of CH_4 oxidation. The free energy profile shown in Figure 7 suggests that the rate-limiting step for the oxidation of methane to acetic acid is the initial activation of CH_4.
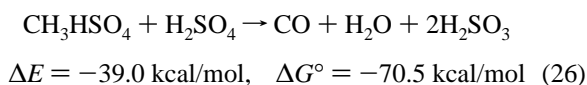
The reaction mechanism shown in Figure 6 does not involve the reduction of Pd^{2+} to Pd^0. However, as noted earlier, Pd deposition is observed during experimental studies.[1,2,15] The calculations reported here suggest that Pd reduction will not occur as a part of the reactions sequence involved in the oxidation of methane to methanol. Therefore, some other species present in the system must be responsible for reducing Pd^{2+}. Experimental work reported by Zerella and Bell has shown that CO produced during the course of the overall reaction can reduce Pd^{2+} to Pd-black.[2,15] Thermodynamic calculations for eqs 24 and 25 show that such processes are favorable, and if these atoms can form small Pd clusters, then the Gibbs free energy change for producing elemental Pd becomes far more favorable. As noted earlier, for the reaction $Pd \rightarrow \tfrac{1}{6}Pd_6$, $\Delta E = -32.6$

$$Pd(\eta^2\text{-}HSO_4)(HSO_4)(H_2SO_4) + CO + H_2O \rightarrow$$
$$Pd(H_2SO_4)_2 + CO_2 + H_2SO_4$$

$$\Delta E = -3.6 \text{ kcal/mol}, \quad \Delta G° = -11.5 \text{ kcal/mol} \quad (24)$$

$$Pd(HSO_4)_2(H_2SO_4)_2 + CO + H_2O \rightarrow Pd(H_2SO_4)_2 + CO_2 +$$
$$2H_2SO_4$$

$$\Delta E = -2.9 \text{ kcal/mol}, \quad \Delta G° = -31.2 \text{ kcal/mol} \quad (25)$$
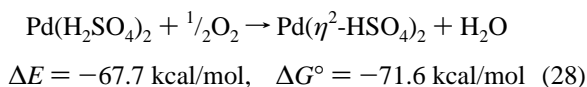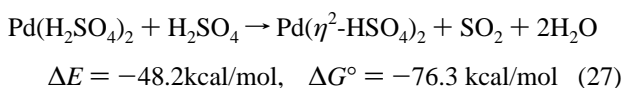
Figure 7. Schematic of the change in electronic energy along a representative pathway for the oxidation of methane to acetic acid. The graph is scaled on the basis of electronic energy (kcal/mol) as shown on the *y*-axis. Standard free energies at 453 K of corresponding structures are given in parentheses. TS2 is the transition state for methane activation. TS3 is the transition state for CO insertion into a Pd—CH₃ bond. TS4 is the transition state for CH₃COHSO₄ elimination from the Pd⁴⁺ center. Dashed lines are shown to indicate portions of the energy profile where the activation barrier had not been calculated.

kcal/mol and $\Delta G^\circ = -23.4$ kcal/mol. These calculations of Pd cluster formation were done with the LANL2DZ basis set, assuming that the reaction occurs in the gas phase. Note that the CO used in above reactions is formed by the oxidation of CH₃HSO₄, which is formed during the reaction cycle. The thermodynamics for such an oxidation is favorable, as shown in eq 26 below.

$$CH_3HSO_4 + H_2SO_4 \rightarrow CO + H_2O + 2H_2SO_3$$

$$\Delta E = -39.0 \text{ kcal/mol}, \quad \Delta G^\circ = -70.5 \text{ kcal/mol} \quad (26)$$

The reoxidation of Pd(0) can occur by one of several processes. Two examples are presented in eqs 27 and 28, one involving H₂SO₄ as the oxidizing agent (eq 27) and one involving O₂ as the oxidizing agent (eq 28).

$$Pd(H_2SO_4)_2 + H_2SO_4 \rightarrow Pd(\eta^2\text{-}HSO_4)_2 + SO_2 + 2H_2O$$

$$\Delta E = -48.2 \text{kcal/mol}, \quad \Delta G^\circ = -76.3 \text{ kcal/mol} \quad (27)$$

$$Pd(H_2SO_4)_2 + {}^1/_2 O_2 \rightarrow Pd(\eta^2\text{-}HSO_4)_2 + H_2O$$

$$\Delta E = -67.7 \text{ kcal/mol}, \quad \Delta G^\circ = -71.6 \text{ kcal/mol} \quad (28)$$

It is evident that Pd(0) can be reoxidized by both H₂SO₄ and O₂, and that the values of ΔG° differ only slightly for eqs 27 and 28. These findings are in qualitative agreement with the experimental work of Zerella et al.[2]

The preceding discussion illustrates the importance of maintaining a proper balance on the concentration of CO in the reaction systems in order to achieve a high yield of acetic acid and retention of Pd²⁺ cations in solution. The insertion of CO into the Pd—CH₃ bond of Pd(HSO₄)(CH₃)(CO)(H₂SO₄), eq 12, is enhanced by an increase in the partial pressure of CO; however, high CO partial pressure favors the reduction of Pd-

(η^2-HSO₄)(HSO₄)(H₂SO₄) and Pd(HSO₄)₂(H₂SO₄)₂ to form Pd-(0) via eqs 24 and 25. These observations are consistent with the experimental findings of Zerella et al.,[2] who found that that the yield of acetic acid passes through a maximum as the partial pressure of CO is increased.

Conclusions

The results of this investigation show that Pd²⁺ cations are stabilized in concentrated sulfuric acid, primarily in the form of Pd(η^2-HSO₄)(HSO₄)(H₂SO₄) and Pd(HSO₄)₂(H₂SO₄)₂. Methane activation occurs primarily via addition of CH₄ across one of the Pd—O bonds of a bisulfate ligand. Insertion of CO into the Pd—CH₃ bond of this species leads to the formation a Pd—COCH₃ species. Direct formation of CH₃HSO₄ or CH₃COHSO₄ via reductive elimination from either Pd(HSO₄)(CH₃)(H₂SO₄)₂ or Pd(HSO₄)(CH₃CO)(H₂SO₄)₂ is predicted to have a high activation barrier. A much more likely route to products involves the oxidation of Pd(HSO₄)(CH₃)(H₂SO₄)₂ and Pd(HSO₄)(CH₃-CO)(H₂SO₄)₂ to form Pd(η^2-HSO₄)(HSO₄)₂(CH₃)(H₂SO₄) and Pd(η^2-HSO₄)(HSO₄)₂(CH₃CO)(H₂SO₄), respectively, which then can readily eliminate CH₃HSO₄ or CH₃COHSO₄, respectively. Acetic acid is then formed by hydrolysis of CH₃COHSO₄, a process which is thermodynamically favored in 96 wt % sulfuric acid. The loss of Pd²⁺ from solution to form Pd(0) or Pd-black is predicted to occur via the reduction with CO. This process is offset, though, by reoxidation of palladium by either H₂SO₄ or O₂. Thus, the maintenance of Pd²⁺ in solution involves proper balancing of reducing and oxidizing species.

Supporting Information Available: Computational details about accuracy of energy calculations; molecular geometries and minimum energy paths; energy calculation worksheet; and complete list of authors for ref 8. This material is available free of charge via the Internet at http://pubs.acs.org.

JA055756I

(24) The activation barriers for this reaction were found with H₂SO₄ ligands replaced by H₂O ligands. This was done to reduce the number of atoms in the growing string method and get the results in a timely manner.